THE JOURNAL OF PHYSICAL CHEMISTRY C

Article

pubs.acs.org/JPCC

High Thermoelectric Performance of Co-Doped Tin Telluride Due to Synergistic Effect of Magnesium and Indium

D. Krishna Bhat* and Sandhya Shenoy U

Department of Chemistry, National Institute of Technology, Karnataka, Surathkal, Mangalore, Karnataka 575025, India

Supporting Information

ABSTRACT: Thermoelectric (TE) materials are considered go-to materials lately in addressing the worldwide energy crisis. We report a study on the effect of co-doping of magnesium and indium in lead-free SnTe both experimentally and theoretically. We show how the resonant levels introduced by indium increase the Seebeck coefficient at lower temperatures and how magnesium enhances the Seebeck at higher temperatures by opening the band gap and decreasing the energy difference between the light and heavy hole valence sub-bands. Synergistically, the effects of band engineering lead to the co-doped sample having high thermoelectric figure of merit (ZT) over a wide range of temperature and record a high power factor of ~42 μW cm^{-1} K^{-2} for SnTe based materials. For the very first time we show the effect of site occupied by the dopant on the electronic structure of the material. The resulting high ZT of 1.5 at 840 K makes SnTe a very suitable material for thermoelectric applications.

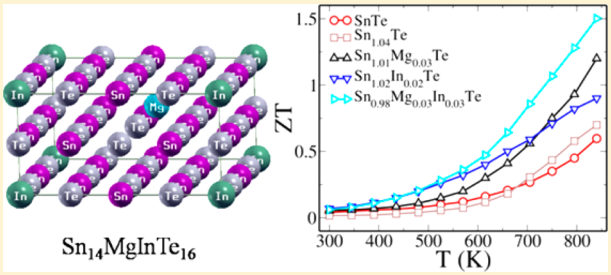

INTRODUCTION

Sustainable power generation is considered an answer by the scientific community to the ever increasing energy crisis, caused by exhaustion of nonrenewable fossil fuel resources, which is a consequence of their abuse.[1] Thermoelectric (TE) materials which can directly and reversibly convert heat into electricity have attracted considerable attention as a pollution free technology.[2] Though all materials have a nonzero thermoelectric effect, in most materials the thermoelectric figure of merit (ZT) is too low to be useful. Although PbTe and its derivative alloys are the best known TE materials, their use is not encouraged due to concerns of environmental toxicity of lead.[3] Hence the need of the day is to identify or develop environment friendly materials with higher thermoelectric efficiency than available at present.[1] The challenge arises due to the conflicting combination of material traits and the well-known interdependence of S, σ, and K.[2] This complicates the efforts to develop strategies for improving a material's average ZT. SnTe, a homologue of PbTe, has a rock salt structure and electronic structure similar to PbTe and is considered safe, but SnTe suffers from a drawback of low ZT due to smaller band gap (~0.18 eV) and higher separation between the valence sub-bands (~0.3 eV) than PbTe.[4] So, in order to improve the ZT of SnTe the band gap has to be widened and the separation between the heavy and light hole valence bands has to be decreased.[5] One more factor which makes SnTe not a suitable candidate for thermoelectrics is its very high carrier concentration. Efforts in this direction have led to doping of SnTe with Mg, Cd, Hg, and Mn so as to bring about opening up of the band gap and valence band convergence; or In to introduce resonance levels.[6−13] The effective way to suppress the excess hole concentration is found to be either by adding electron donor dopants like I or by self-compensation of Sn.[6,7] Recently, co-doping of Cd−In and Ag−In has also been tried to enhance the thermoelectric performance of SnTe via band engineering.[14,15] Yet another way to improve the ZT of SnTe or in general metal chalcogenides is by reducing the thermal conductivity by enhanced alloy scattering and inclusion of various nanostructures.[1,3]

In order to design a material with enhanced thermoelectric efficiency it is essential to understand the chemistry and physics of the material. We thought it would be worthwhile to investigate the effect of co-doping of magnesium and indium in SnTe, as Mg is believed to act similar to Cd and Hg.[6] Though there are reports of Mg-doped SnTe and PbTe, they do not explain in detail the effect of the site occupied by Mg on the thermoelectric properties precisely.[6,16−18] It is known that when Mg is doped in either SnTe or PbTe, it opens up the band gap of the parent material causing reduction of bipolar diffusion at higher temperatures.[6,16] The light hole band at the L point drops down in its energy and the difference between the energy of this band and the heavy hole valence band at the Σ point decreases, leading to an increase in Seebeck values. Herein we make an effort to explain the effect of the site occupied by the dopant atom on the thermoelectric properties using density functional theory (DFT) first-principles calculations supported by the experimental results. We also show how co-doping of Mg and In results in enhancement of the figure of merit ZT due to the complementary role of Mg and In in modifying the electronic structure of SnTe. The synergistic

Received: January 27, 2017
Revised: March 5, 2017
Published: March 27, 2017

DOI: 10.1021/acs.jpcc.7b00870
J. Phys. Chem. C 2017, 121, 7123−7130

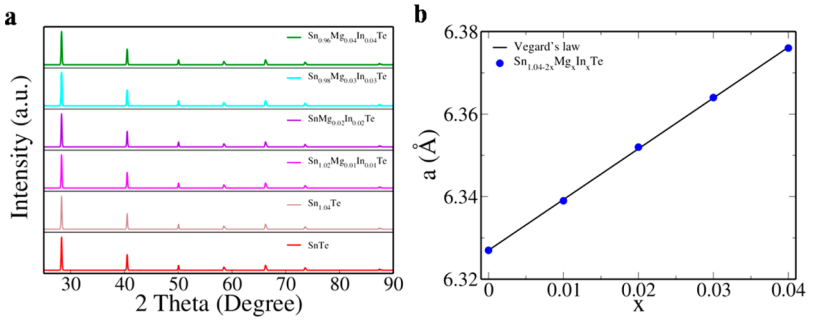

Figure 1. (a) pXRD pattern and (b) variation of lattice parameter a versus dopant concentration x in $Sn_{1.04-2x}Mg_xIn_xTe$.

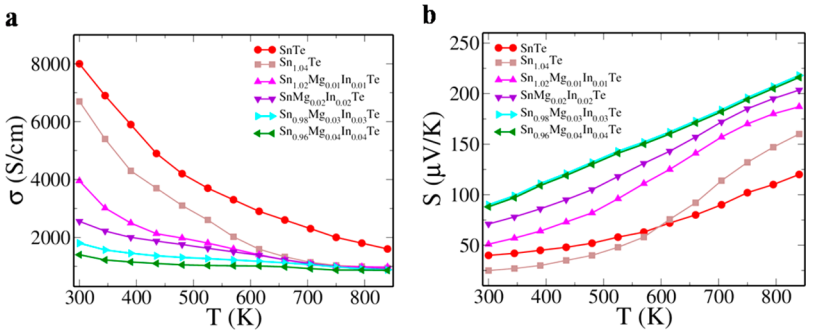

Figure 2. Variation of (a) electrical conductivity and (b) Seebeck coefficient with temperature in $Sn_{1.04-2x}Mg_xIn_xTe$.

action in the case of Mg and In co-doping is found to be higher than that in the previously reported co-dopants and has produced a record high power factor and ZT in SnTe based materials.

RESULTS AND DISCUSSION

The sample $Sn_{1.04-2x}Mg_xIn_xTe$ was prepared by modified self-propagating high temperature synthesis (SHS) and spark plasma sintering (SPS) process. This combination of the SHS and SPS process is used for the very first time for the synthesis of SnTe based materials. Currently used techniques to optimize the thermoelectric properties of SnTe are decreasing the carrier concentration, improving the electronic transport properties, or reducing the total thermal conductivity.[1] These largely depend on the solubility of the dopant in the parent matrix, and hence increasing the solubility is highly important.[1,11] In conventional solid solution alloying the solubility is limited by equilibrium phase diagram. But in the case of SHS, higher solid solubility can be attained at room temperature by a nonequilibrium process. The intense heat released during the exothermic reaction makes the reaction self-propagating. The method is simple, quick, cost-effective, and scalable for large-scale production. SnTe is known to have intrinsic Sn vacancies, which is one of the reasons which make it not a good material for thermoelectric applications. Self-compensation of Sn has been proven to be a good way to reduce the carrier concentration in pristine SnTe.[6,7] Herein we prepare the samples by self-compensating the vacancies, achieving an optimized concentration of $Sn_{1.04}Te$, and we then co-dope it with Mg and In.

The as-synthesized compound was characterized by pXRD. The diffraction pattern revealed in Figure 1a could be indexed to cubic NaCl structure with space group $Fm3m$. The formation of a single phase was confirmed as no other peaks of impurity were observed within the detection limits. This shows that SHS process can be successfully used to prepare single phase materials with lower energy consumption and easier fabrication. We see that the calculated lattice parameter value (a) gradually increases with increase in concentration of Mg and In during co-doping which is contradictory to the previously reported case of Mg doped SnTe.[6] InTe has a lattice parameter approximately similar to that of SnTe (~6.32 Å), and hence doping In does not have much effect on the lattice parameter. Hence, any change in lattice parameter is due to the introduction of Mg. In the earlier report, the decrease in lattice parameter with introduction of Mg in SnTe was believed to be the consequence of the smaller radius of Mg ions compared to Sn ions.[6] MgTe, when it crystallizes in a rock salt site, has a lattice parameter of ~5.92 Å, and when it crystallizes in a zinc blende site, has a lattice parameter of ~6.45 Å.[17] Therefore, if Mg occupies the rock salt site then the lattice parameter should have decreased, while in the zinc blende site it should have increased. Hence the linear increase in the lattice parameter with dopant concentration until 4 mol % shows that Mg goes into zinc blende site and also follows Vegard's law (Figure 1b). The occupancy of Mg in the zinc blende site is further confirmed by DFT calculations in later sections. In the previous reports of Mg-doped PbTe, there are huge contradictions in the solubility limit of Mg in PbTe apart from the trend in the lattice parameter.[16−18] Though in one of the reports, they claim that Mg goes into the zinc blende site, they do not exactly provide direct evidence.[17] If it did go into the zinc blende site, then the lattice parameter should have remained almost constant, as PbTe has a lattice constant similar to that of MgTe (zinc blende). The reason for the initial decrease is said to be the decrease in radius as Mg substitutes Pb in the lattice. The further increase in lattice constant is said to be due to expulsion of Na from the matrix. However, for the same set of materials and concentration, the subsequently reported paper gives a different trend with no mention of Na

DOI: 10.1021/acs.jpcc.7b00870
J. Phys. Chem. C 2017, 121, 7123−7130

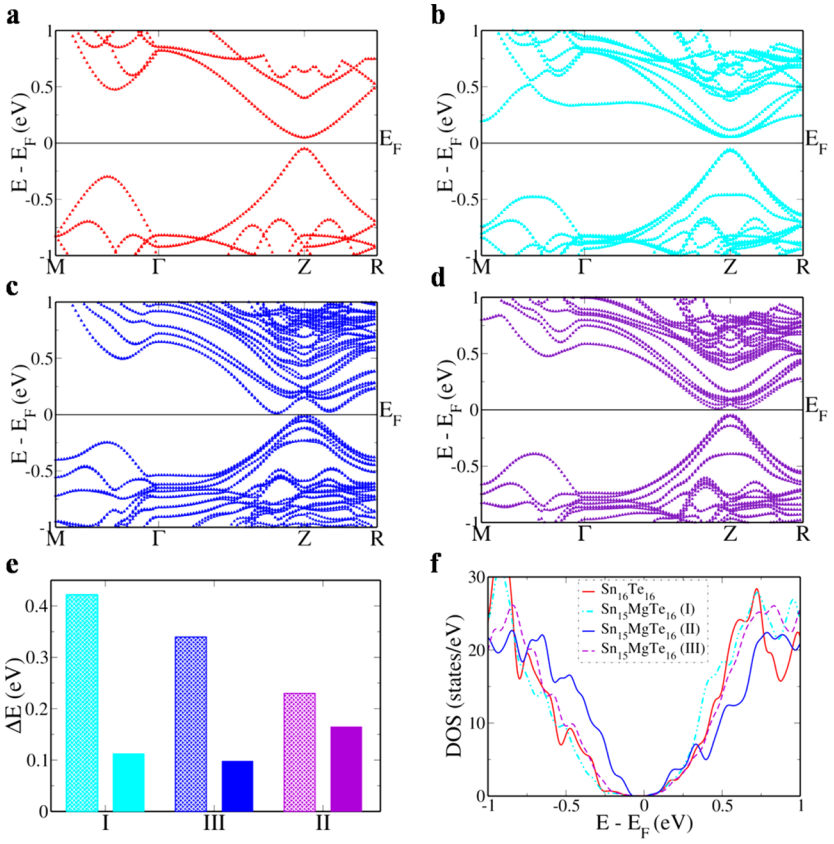

Figure 3. Electronic structure of (a) $Sn_{16}Te_{16}$, (b) $Sn_{15}MgTe_{16}$ (Configuration I), (c) $Sn_{15}MgTe_{16}$ (Configuration II), (d) $Sn_{15}MgTe_{16}$ (Configuration III), (e) Band gap at Z point (solid bar) and difference in energy between light and heavy hole valence subbands (designed bar) occurring at Z point and M + δ point along the M → Γ direction, respectively, in the tetragonal supercell of $Sn_{15}MgTe_{16}$ for three different configurations, (f) Density of states plot for $Sn_{16}Te_{16}$, $Sn_{15}MgTe_{16}$ (configurations I–III).

expulsion and a different solubility limit.[16] The present work gives insights about how the contradictions can be looked at and solved.

Thermoelectric transport properties as a function of temperature were studied in the range 300 to 900 K. We observe that co-doping of Mg and In decreases the electrical conductivity values with increase in concentration of the dopants. Also, for a given concentration of dopant the electrical conductivity values decrease with increase in temperature (Figure 2a). This decrease in electrical conductivity values with increase in temperature shows the degenerate nature of the semiconducting materials.[6] We see that the values of electrical conductivity of the Mg–In co-doped samples are intermediate compared to the previously reported SnTe samples singly doped with Mg and In.[6,11,12] The room temperature electrical conductivity decreases from 6700 S cm^{-1} to 1400 S cm^{-1} as x increases from 0 to 4 mol % in $Sn_{1.04-2x}Mg_xIn_xTe$. The carrier concentration of SnTe reduces from 3.5 × 10^{20} cm^{-3} to 2 × 10^{20} cm^{-3} on self-compensation of Sn vacancies as established in the previous report.[7] The carrier concentration increases to 4.6 × 10^{20} cm^{-3} as the x increases to 3 mol % in $Sn_{1.04-2x}Mg_xIn_xTe$.

Figure 2b reveals that the Seebeck coefficients have positive values and they show an increasing trend with increase in temperature and dopant concentration. The positive value of Seebeck coefficient indicates the p-type conduction indicating that holes are the majority carriers. The self-compensated sample shows a maximum value of Seebeck coefficient of 160 $\mu V\ K^{-1}$ around 840 K, while for the co-doped sample it increases to 218 $\mu V\ K^{-1}$ when x = 0.03 in $Sn_{1.04-2x}Mg_xIn_xTe$ much higher than the value of 120 $\mu V\ K^{-1}$ for pristine SnTe. This observed enhancement of Seebeck values is due to two reasons, the first being the introduction of resonance levels by In which is known to increase the Seebeck values at lower temperatures by increasing the band effective mass m_b*.[1,12−15] At higher temperatures the Seebeck value increases as a result of Mg doping. Introduction of Mg brings about the decrease in the energy separation between the light hole and heavy hole valence subbands.[6] Due to this type of convergence of valence bands, the number of equivalent degenerate valleys of band structure (N_v) increases from 4 to 16, as heavy hole band contributes N_v of 12 to the already existing N_v of 4 contributed by the light hole bands.[1] Introduction of resonance levels by In and valence band convergence by Mg is an effective way to increase the Seebeck coefficient which is directly proportional to carrier effective mass m*, which in turn is directly proportional to m_b* and $(N_v)^{2/3}$. The co-doped sample has Seebeck values higher than the individually doped samples reported in previous literature throughout the temperature range due to the synergistic action of resonance levels and valence band convergence, which acts at lower and higher temperatures, respectively.[6,12,13] In addition to this, the introduction of Mg increases the band gap, which decreases the bipolar conduction at higher temperatures, which otherwise would have had a detrimental effect on Seebeck values at higher temperatures as minority carriers would have offset the effect of majority carriers causing Seebeck values to decrease.

DOI: 10.1021/acs.jpcc.7b00870
J. Phys. Chem. C 2017, 121, 7123−7130

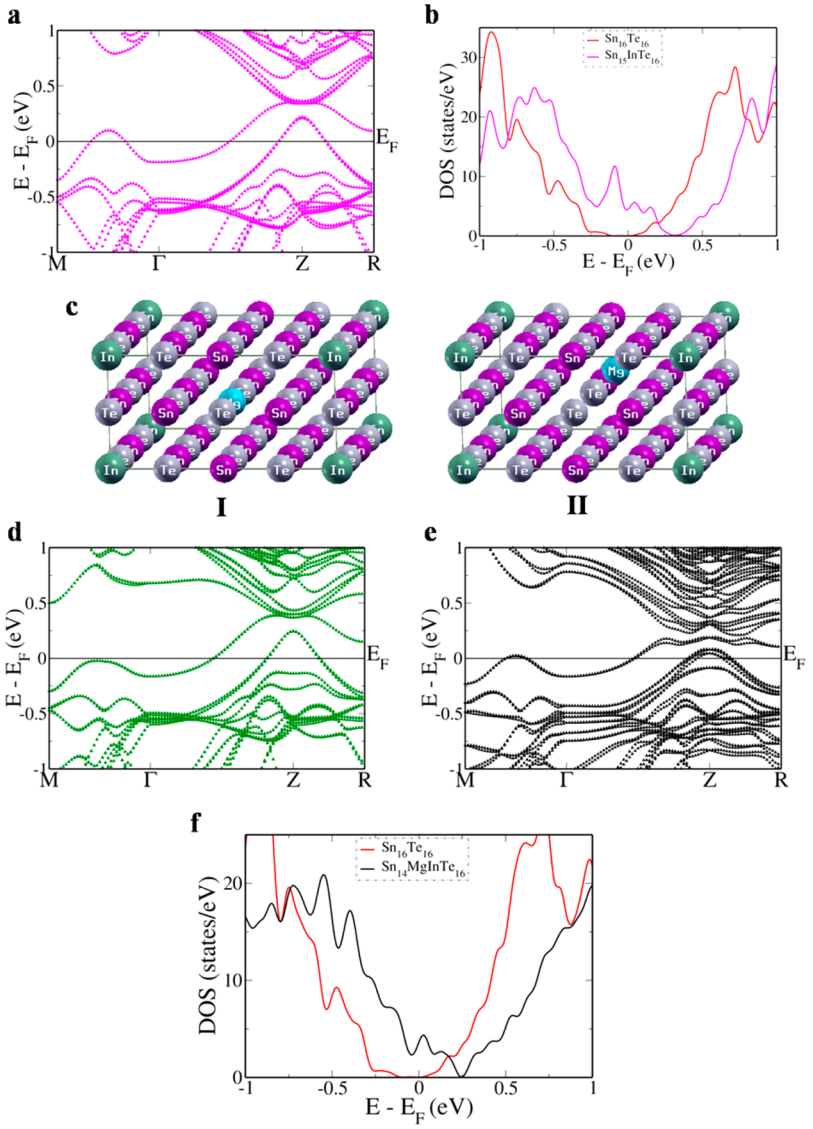

Figure 4. Electronic structure of (a) $Sn_{15}InTe_{16}$ (In in rock salt site). (b) Density of states plot for $Sn_{16}Te_{16}$, $Sn_{15}InTe_{16}$. (c) Crystal structures of $Sn_{14}MgInTe_{16}$ (I - Mg in rock salt site, II -Mg in zinc blende site). (d) Electronic structure of $Sn_{14}MgInTe_{16}$ (Configuration I), (e) Electronic structure of $Sn_{14}MgInTe_{16}$ (Configuration II), (f) Density of states plot for $Sn_{16}Te_{16}$, $Sn_{14}MgInTe_{16}$ (Configuration II).

To explain the experimentally observed increase in Seebeck values, we carry out DFT calculations on pristine Mg, In individually doped and Mg−In co-doped SnTe. Though the SnTe primitive cell contains two atoms, the simulations were carried out using a 32 atom supercell to achieve ∼6.25 mol % doping concentration. MgTe is known to crystallize in a zinc blende structure with space group *F*43*m* in addition to the rock salt structure. Hence, the electronic structures were determined for both cases by placing the dopant in appropriate sites (Figure S1). It is a well-known fact that SnTe has a low principle band gap of ∼0.18 eV at the L point and a energy separation of ∼0.30 eV between the light and heavy hole valence subbands occurring at L and Σ points, respectively. The electronic structure reveals a band gap of ∼0.098 eV at the Z point consistent with the experimental values considering the typical underestimation caused in DFT based calculations (Figure 3a). When a supercell is constructed, the Brillouin zone folds accordingly and hence the states at the L point in the primitive cell correspond to the states at the Z point in the supercell, while the Σ point where the heavy hole valence band occurs folds onto the M + δ point along the M → Γ direction in the tetragonal supercell.

In the previously reported papers where the effect of MgX on metal chalcogenides are shown, the crystal structure adopted by the MgX and the reason for the same is not explicitly discussed.[6,16−18] Hence, in order to get a clear picture first we put one Mg in the rock salt site (corresponding to Wyckoff coordinate of 000 in the primitive cell) of Sn (configuration I) and determine its electronic structure (Figure 3b). We see that though the band gap increases slightly to ∼0.112 eV, the valence subbands instead of undergoing convergence undergo divergence. The energy gap increases to ∼0.422 eV. This should in fact cause a decrease in the Seebeck coefficient values with Mg doping which is contradictory to the experimental results we observe. Therefore, we substituted one Mg in the zinc blende site (corresponding to Wyckoff coordinate of 0.25 0.25 0.25 in the primitive cell) for one Sn atom (configuration II) and the obtained electronic structure (Figure 3c) revealed that the band gap at the Z point increased to ∼0.165 eV compared to ∼0.098 eV of the pristine and the energy gap

DOI: 10.1021/acs.jpcc.7b00870
J. Phys. Chem. C 2017, 121, 7123−7130

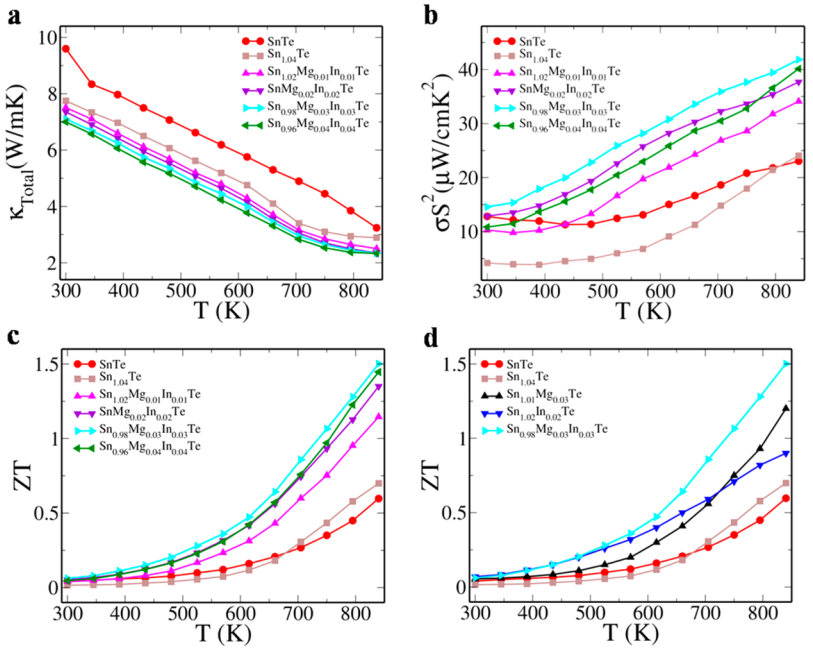

Figure 5. Variation of (a) total thermal conductivity, (b) power factor, (c) ZT with temperature in $Sn_{1.04-2x}Mg_xIn_xTe$. (d) Comparison of variation of ZT with temperature of samples with optimized concentration.

between the light hole and heavy hole valence band decreased to ∼0.230 eV. This value of convergence is much higher and significant compared to the decrease in the gap by ∼0.005 eV in a previously reported Mg doped SnTe for the same concentration (∼6.25 mol %).[6] The W-shaped band appearing in the conduction band of the doped sample is due to the positional effect. To confirm this, we put Mg halfway between the rock salt site and the zinc blende site (configuration III). The electronic structure (Figure 3d) revealed that the energy gap between the valence subbands is halfway between those of configurations I and II (Figure 3e) and the depth of the W-shaped conduction band is less prominent than in the case of electronic structure of configuration II. In this case, even though the band gap remained the same as that of the pristine sample, the energy difference between the valence subbands was ∼0.340 eV showing an increase from the pristine sample as well as that from the case of configuration II. The density of states plot (Figure 3f) shows that in configuration I the density of states is lower than the pristine SnTe at the top of the valence band, while configuration II causes an increase in the density of states which causes an increase in the Seebeck values; whereas for configuration III we see that the density of states slightly increases near the top of the valence band compared to configuration I, indicating slightly better convergence than the latter. This confirms that Mg goes into the zinc blende site and not the rock salt site. We also see that the difference in the total energy when Mg is put in the rock salt site and the zinc blende site is ∼1.67 eV.

Similarly, In was placed in the rock salt site and the electronic structure was determined (Figure 4a). Clearly, we see the resonance level introduced by the introduction of In. The same is confirmed in the density of states plot (Figure 4b) in the form of humps just after the Fermi level within the valence band. The resonant states are believed to be formed by the overlap of In s and Te p orbitals in their antibonding state near the edge of the band gap.[13] It is a well-known fact that the extent to which dopant orbitals contribute to the valence band determines the tuning of the band gap. In the case of the In-doped SnTe sample we see that In orbitals are localized in a narrow energy range of the valence band. The region where the contribution of In orbital is highest appears as a hump in the DOS plot, and in the electronic structure, the same is seen as a split off band increased in energy.[14,15] The higher the increase in energy, the sharper the peak in the DOS plot is. Although there is a difference of opinion on whether In also causes valence band convergence in SnTe or not, we see that in addition to introduction of resonance level, In also causes convergence of the valence subbands leading to an energy difference of about ∼0.243 eV between the valence subbands.[13−15] However, this convergence is less compared to that caused by Mg for the same concentration of doping. However, when In is in the zinc blende site the resonance level appears in the conduction band and hence shows n-type behavior similar to In doping in PbTe (Figure S2a).[12] We know that In in SnTe is a p-type dopant, which clearly indicates that In occupies the rock salt site.[12] Surprisingly in the case of PbTe, In in the rock salt site shows n-type behavior (Figure S2b). Hence, we can generalize that the site and the behavior are specific to a particular compound.

Since we knew our material was p-type, we fixed the position of In to the rock salt site and varied the position of Mg in the co-doped crystal (Figure 4c). The electronic structure where Mg is in the rock salt site shows the resonance level due to the presence of In in the co-doped sample, but the band gap does not open up and also the energy difference between the valence subbands increases to ∼0.390 eV (Figure 4d), whereas the electronic structure of the co-doped sample with Mg in the zinc blende site reveals an energy gap between the valence subbands of about ∼0.161 eV. We also see that at the Z point the band gap is about ∼0.230 eV with the resonance level passing at the center of the gap (Figure 4e). The presence of the resonance level and the valence band convergence is indicated in the DOS plot in the form of a well-defined peak near the Fermi level and the increase in the density of states near the top

DOI: 10.1021/acs.jpcc.7b00870
J. Phys. Chem. C 2017, 121, 7123−7130

of the valence band (Figure 4f). This shows that when In is co-doped with Mg the performance of the material becomes better than that of Mg and In alone.

Temperature dependence of the total thermal conductivity is as shown in Figure 5a. The total thermal conductivity of the co-doped sample decreases with increase in doping concentration as well as temperature. The temperature dependent heat capacity data is given in Figure S3. We observe that the co-doped samples have thermal conductivity less than that of the undoped sample. The thermal conductivity (total) contains a contribution of lattice, electronic, and bipolar thermal conductivities. Usually the lattice thermal conductivity is determined by subtracting the electronic part from the total thermal conductivity.[6] The electronic thermal conductivity in turn is determined using the Wiedemann−Franz law (electronic thermal conductivity = $L\sigma T$, where L is Lorenz number, σ is electrical conductivity, and T is absolute temperature). However, recent reports suggest that when multiple bands coexist at the Fermi level, the carriers move from one valley into another by means of a complex intervalley scattering.[15] This causes large amount of heat to transfer which cannot be determined by the L value. In our present co-doped sample since we see a convergence of valence bands there is a possibility of intervalley scattering. Hence, we have not determined the lattice thermal conductivity, but it is safe to assume that the decrease in the total thermal conductivity with increase in doping concentration is due to the increase in the atomic point defects due to elemental substitution. These point defects are known to scatter the phonons causing additional thermal resistance and lowering of the lattice thermal conductivity.[1] On the other hand, the bipolar conductivity arises due to the ambipolar diffusion of electrons and holes. At higher temperatures, the minority carriers increase the thermal conductivity values in addition to decreasing the value of Seebeck coefficient due to bipolar diffusion. The diffusing electron hole pairs become an additional component in this case. In our present work as Mg concentration increases in the doped samples the band gap increases; as a result, there is no scope for bipolar diffusion at higher temperatures.[6,16]

It is observed that the power factors obtained in the case of Mg−In co-doped samples are higher compared to that of the self-compensated SnTe throughout the temperature range and doping concentration range reported in this study. The dependence of the power factor on the temperature is shown in Figure 5b. The increase in the value of Seebeck with the increase in dopant concentration is responsible for the increase in the power factor. We see that the power factor increases to ∼42 μW cm^{-1} K^{-2} when x = 0.03 at 840 K. This is the highest reported power factor for SnTe based materials, even higher than ∼32 μW cm^{-1} K^{-2} reported recently for Ag−In co-doped SnTe which held the record by far.[15] Co-doping of Mg and In in self-compensated SnTe has an enormous effect on the ZT values, which is much more than the previously reported cases of co-doping of Cd−In and Ag−In in SnTe or individually doped Mg, Cd, Hg, Mn, In, Ca, Ga, Sr in SnTe, some of which even employ nanostructuring.[6−12,14,15,19−21] A comparison of power factors and ZT of some of the SnTe based materials is given in the Figure S4. The ZT values in the case of $Sn_{1.04-2x}Mg_xIn_xTe$ increased with increase in doping concentration (from x = 0.00 to x = 0.04) and a maximum ZT of ∼1.5 at 840 K and a ZT_{avg} of ∼0.6 considering 300 and 840 K as cold and hot ends were obtained for x = 0.03 in $Sn_{1.04-2x}Mg_xIn_xTe$ (Figure 5c). We see that for x = 0.03 in $Sn_{1.04-2x}Mg_xIn_xTe$ the co-doped sample has higher ZT than the pristine, self-compensated, and even the optimized individually doped sample (Figure 5d). The maximum ZT of ∼1.5 suggests that this material has great promise for further study.

CONCLUSIONS

We report a study on the effect of co-doping of Mg and In in SnTe both experimentally through synthesis, characterization, and study of properties of the material and theoretically through first-principles density functional theory electronic structure calculations. For the very first time we use a combination of SHS and SPS process to synthesize Mg−In co-doped SnTe. We see that In introduces resonant levels increasing the Seebeck coefficient at lower temperatures. Mg on the other hand increases the band gap and decreases the energy difference between the light and heavy hole valence sub-bands, suppressing the bipolar thermal conduction at higher temperature and enhancing the Seebeck coefficient values. All these effects synergistically led to a record high power factor of ∼42 μW cm^{-1} K^{-2} and high ZT over a wide range of temperature in the co-doped sample. For the very first time we show that Mg occupies a zinc blende site (and not rock salt site), in SnTe, and is responsible for the increase in the band gap and degeneracy of valence sub-bands. The resulting high ZT of 1.5 at 840 K and ZT_{avg} of ∼0.6 considering 300 and 840 K as cold and hot ends make SnTe a very suitable material for thermoelectric applications.

METHODS

Computational Details. The electronic structure and density of states of SnTe, Mg doped SnTe, In doped SnTe, and Mg−In co-doped SnTe were determined using Quantum Espresso package by DFT calculations.[22] Since Sn and Te have high atomic numbers, the effect of spin orbit coupling cannot be neglected. Hence, fully relativistic ultrasoft pseudopotentials were used to elucidate the realistic electronic structure in the calculations. A Generalized Gradient Approximation (GGA) with parametrized functional of Perdew, Burke, and Erzenhoff (PBE) was used to approximate the exchange-correlation energy functional.[23] Simulation of substitutional doping was done using a 2 × 2 × 1 supercell of primitive rock salt SnTe structure with $Fm3m$ space group symmetry. A uniform grid containing 4000 k-points was used to sample integrations over the Brillouin-zone of the supercell containing 32 atoms for electronic structure calculations. An energy cutoff of 50 Ry and charge density cutoff of 400 Ry was used to truncate the plane wave basis representing wave functions. Electronic structure was determined along high symmetry lines (M - Γ - Z - R) in the Brillouin zone and Gaussian smearing was used to smear the discontinuity in the occupation numbers of electronic states with a width of 0.01 eV.

Synthesis. Tin, tellurium, magnesium, and indium were procured from Alfa Aesar of high purity (99.99+ %) and were used for synthesis without further purification. They were thoroughly mixed together according to their nominal composition using a mortar and pestle. They were cold-pressed in a dye under 5 MPa pressure into a pellet. The pellet was then sealed under vacuum (10^{-5} Torr) in a silica tube. The self-propagating high temperature synthesis (SHS) process was initiated by igniting the pellet using a hand torch. The combustion wave passed through it within seconds. The product thus obtained was again ground using mortar and

DOI: 10.1021/acs.jpcc.7b00870
J. Phys. Chem. C 2017, 121, 7123−7130

pestle. It was later densified using spark plasma sintering (SPS) method (SPS-211LX, Fuji Electronic Industrial Co., Ltd.) at 500 °C in a graphite dye in vacuum. The resulting sample was further subjected to annealing treatment at 900 °C for 24 h.

X-ray Diffraction Measurements. Powder X-ray diffraction (pXRD) of the synthesized samples were recorded on Bruker D8 diffractometer using a Cu K_α (λ = 1.5406 Å) radiation.

Transport Properties. The samples were cut in ∼2 × 2 × 8 mm^3 dimensions (parallelepiped shape) and in ∼8 mm diameter and ∼2 mm thickness (coin shape) for conductivity and thermal diffusivity measurements. ULVAC-RIKO ZEM-3 instrument system was used to determine electrical conductivity and Seebeck coefficient under helium atmosphere in the temperature range of 300−900 K. The conductivity measurements were done in the longer direction. Carrier concentrations were determined at 300 K with a PPMS system using Hall coefficient measurements. The carrier concentration, n, was estimated from the formula $n = 1/eR_H$, where e is the electronic charge. Thermal diffusivity was measured in the temperature range from 300 to 900 K using laser flash diffusivity method in a Netzsch LFA-457. The total thermal conductivity was calculated by the product of thermal diffusivity, temperature dependent heat capacity (derived using standard sample (pyroceram) in LFA-457), and the density of the sample. The density of the pellets obtained was ∼97% of the theoretical density.

■ ASSOCIATED CONTENT

Supporting Information

The Supporting Information is available free of charge on the ACS Publications website at DOI: 10.1021/acs.jpcc.7b00870.

Crystal structures of $Sn_{1-x-y}Mg_xIn_yTe$. Electronic structures of In (in zinc blende site) doped SnTe and In (in rock salt site) doped PbTe. Temperature dependent heat capacity data. Comparison of power factors and ZT values of SnTe based materials. (PDF)

■ AUTHOR INFORMATION

Corresponding Author

*E-mail: denthajekb@gmail.com.

ORCID

D. Krishna Bhat: 0000-0003-0383-6017

Notes

The authors declare no competing financial interest.

■ ACKNOWLEDGMENTS

The authors gratefully acknowledge SERB, Govt. of India for financial support in the form of an R&D project grant.

■ REFERENCES

(1) Tan, G.; Zhao, L. D.; Kanatzidis, M. G. Rationally Designing High-Performance Bulk Thermoelectric Materials. *Chem. Rev.* **2016**, *116*, 12123−12149.

(2) Snyder, G. J.; Toberer, E. S. Complex Thermoelectric Materials. *Nat. Mater.* **2008**, *7*, 105−114.

(3) Zhou, M.; Snyder, G. J.; Li, L.; Zhao, L. D. Lead-Free Tin Chalcogenide Thermoelectric Materials. *Inorg. Chem. Front.* **2016**, *3*, 1449−1463.

(4) Rogers, L. M. Valence Band Structure of SnTe. *J. Phys. D: Appl. Phys.* **1968**, *1*, 845.

(5) Pei, Y.; Wang, H.; Snyder, G. J. Band Engineering of Thermoelectric Materials. *Adv. Mater.* **2012**, *24*, 6125−6135.

(6) Banik, A.; Shenoy, U. S.; Anand, S.; Waghmare, U. V.; Biswas, K. Mg Alloying in SnTe Facilitates Valence Band Convergence and Optimizes Thermoelectric Properties. *Chem. Mater.* **2015**, *27*, 581−587.

(7) Tan, G.; Zhao, L. D.; Shi, F.; Doak, J. W.; Lo, S. H.; Sun, H.; Wolverton, C.; Dravid, V. P.; Uher, C.; Kanatzidis, M. G. High Thermoelectric Performance of p-type SnTe via a Synergistic Band Engineering and Nanostructuring Approach. *J. Am. Chem. Soc.* **2014**, *136*, 7006−7017.

(8) Tan, G.; Shi, F.; Doak, J. W.; Sun, H.; Zhao, L. D.; Wang, P.; Uher, C.; Wolverton, C.; Dravid, V. P.; Kanatzidis, M. G. Extraordinary Role of Hg in Enhancing the Thermoelectric Performance of p-type SnTe. *Energy Environ. Sci.* **2015**, *8*, 267−277.

(9) Tan, G.; Shi, F.; Hao, S.; Chi, H.; Bailey, T. P.; Zhao, L. D.; Uher, C.; Wolverton, C.; Dravid, V. P.; Kanatzidis, M. G. Valence Band Modification and High Thermoelectric Performance in SnTe Heavily Alloyed with MnTe. *J. Am. Chem. Soc.* **2015**, *137*, 11507−11516.

(10) He, J.; Tan, X.; Xu, J.; Liu, G. Q.; Shao, H.; Fu, Y.; Wang, X.; Liu, Z.; Xu, J.; Jiang, H.; et al. Valence Band Engineering and Thermoelectric Performance Optimization in SnTe by Mn-Alloying via a Zone Melting Method. *J. Mater. Chem. A* **2015**, *3*, 19974−19979.

(11) Liang, T.; Su, X.; Tan, X.; Zheng, G.; She, X.; Yan, Y.; Tang, X.; Uher, C. Ultra-Fast Non-Equilibrium Synthesis and Phase Segregation in $In_xSn_{1-x}Te$ Thermoelectrics by SHS-PAS Processing. *J. Mater. Chem. C* **2015**, *3*, 8550−8558.

(12) Zhang, Q.; Liao, B.; Lan, Y.; Lukas, K.; Liu, W.; Esfarjani, K.; Opeil, C.; Broido, D.; Chen, G.; Ren, Z. High Thermoelectric Performance by Resonant Dopant Indium in Nanostructured SnTe. *Proc. Natl. Acad. Sci. U. S. A.* **2013**, *110*, 13261−13266.

(13) Tan, X. J.; Liu, G. Q.; Xu, J. T.; Shao, H. Z.; Jiang, J.; Jiang, H. C. Element-Selective Resonant State in M-doped SnTe (M = Ga, In, and Tl). *Phys. Chem. Chem. Phys.* **2016**, *18*, 20635−20639.

(14) Tan, G.; Shi, F.; Hao, S.; Chi, H.; Zhao, L. D.; Uher, C.; Wolverton, C.; Dravid, V. P.; Kanatzidis, M. G. co-doping in SnTe: Enhancement of Thermoelectric Performance through Synergy of Resonance Levels and Band Convergence. *J. Am. Chem. Soc.* **2015**, *137*, 5100−5112.

(15) Banik, A.; Shenoy, U. S.; Saha, S.; Waghmare, U. V.; Biswas, K. High Power Factor and Enhanced Thermoelectric Performance of $SnTe-AgInTe_2$: Synergistic Effect of Resonance Level and Valence Band Convergence. *J. Am. Chem. Soc.* **2016**, *138*, 13068−13075.

(16) Zhao, L. D.; Wu, H. J.; Hao, S. Q.; Wu, C. I.; Zhou, X. Y.; Biswas, K.; He, J. Q.; Hogan, T. P.; Uher, C.; Wolverton, C.; et al. All-Scale Hierarchical Thermoelectrics: MgTe in PbTe Facilitates Valence Band Convergence and Suppresses Bipolar Thermal Transport for High Performance. *Energy Environ. Sci.* **2013**, *6*, 3346−3355.

(17) Ohta, M.; Biswas, K.; Lo, S. H.; He, J.; Chung, D. Y.; Dravid, V. P.; Kanatzidis, M. G. Enhancement of Thermoelectric Figure of Merit by the Insertion of MgTe Nanostructures in p-type PbTe Doped with Na_2Te. *Adv. Energy Mater.* **2012**, *2*, 1117−1123.

(18) Pei, Y.; Lalonde, A. D.; Heinz, N. A.; Shi, X.; Iwanaga, S.; Wang, H.; Chen, L.; Snyder, G. J. Stabilizing the Optimal Carrier Concentration for High Thermoelectric Efficiency. *Adv. Mater.* **2011**, *23*, 5674−5678.

(19) Al Rahal Al Orabi, R.; Mecholsky, N. A.; Hwang, J.; Kim, W.; Rhyee, J. S.; Wee, D.; Fornari, M. Band Degeneracy, Low Thermal Conductivity, and High Thermoelectric Figure of Merit in SnTe-CaTe Alloys. *Chem. Mater.* **2016**, *28*, 376−384.

(20) Al Rahal Al Orabi, R.; Hwang, J.; Lin, C. C.; Gautier, R.; Fontaine, B.; Kim, W.; Rhyee, J. S.; Wee, D.; Fornari, M. Ultra-Low Lattice Thermal Conductivity and Enhanced Thermoelectric Performance in SnTe:Ga Materials. *Chem. Mater.* **2017**, *29*, 612−620.

(21) Zhao, L. D.; Zhang, X.; Wu, H.; Tan, G.; Pei, Y.; Xiao, Y.; Chang, C.; Wu, D.; Chi, H.; Zheng, L.; et al. Enhanced Thermoelectric Properties in the Counter-Doped SnTe System with Strained Endotaxial SrTe. *J. Am. Chem. Soc.* **2016**, *138*, 2366−2373.

DOI: 10.1021/acs.jpcc.7b00870
J. Phys. Chem. C 2017, 121, 7123−7130

(22) Giannozzi, P.; Baroni, S.; Bonini, N.; Calandra, M.; Car, R.; Cavazzoni, C.; Ceresoli, D.; Chiarotti, G. L.; Cococcioni, M.; Dabo, I.; et al. Quantum Espresso: a Modular and Open-Source Software Project for Quantum Simulations of Materials. *J. Phys.: Condens. Matter* **2009**, *21*, 395502.
(23) Perdew, J. P.; Burke, K.; Ernzerhof, M. Generalized Gradient Approximation Made Simple. *Phys. Rev. Lett.* **1996**, *77*, 3865−3868.

DOI: 10.1021/acs.jpcc.7b00870
J. Phys. Chem. C 2017, 121, 7123−7130